Bulgarian Chemical Communications, Volume 55, Issue 1 (pp. 13-20) 2023 *DOI: 10.34049/bcc.55.1.5402*

In vitro corrosion behavior, mechanical properties of nano biocomposite coated 316L SS for dental applications

S. Mohandoss[1*], S. Suja[2], S.P. Srinivasan[1], S. Chitradevi[3], B. Venkatachalapathy[4], T. M Sridhar[5]

[1]*Department of Chemistry, Rajalakshmi Engineering College, Chennai - 602105, India*
[2]*Department of Chemistry, S.A. Engineering College, Chennai - 600077, India*
[3]*Department of Chemistry, Rajalakshmi Institute of Technology, Chennai - 600124, India*
[4,] *Karpagam Academy of Higher Education, Coimbatore - 641021, India*
[5]*Department of Analytical Chemistry, University of Madras, Chennai - 600085, India*

Received: April 27, 2021; Revised: December 14, 2022

In the present study, 316L stainless steel (SS) surface was modified with nano yttria stabilized zirconia (YSZ) and nano chitosan by electrophoretic deposition (EPD) and dip coating method. Further, characterizations using XRD, FTIR, FESEM with EDAX confirmed the structural and morphological properties of the coated samples. The corrosion behavior of nano chitosan/YSZ coated 316L SS samples in artificial saliva medium with different concentrations of citric acid and tartaric acid was studied using open circuit potential (OCP) time measurements, Nyquist impedance and cyclic potentiodynamic polarization studies (CPP). The composition and the morphology of nano chitosan/YSZ coated 316L SS samples were analyzed by SEM with EDAX and XRD. The cell viability of nano chitosan/YSZ coated 316L SS and uncoated 316L SS samples was analyzed by the MTT assay method.

Keywords: 316L SS, YSZ, Chitosan, EPD, Dip coating, Electrochemical performance

INTRODUCTION

Recently, dental implants are made of materials such as metals, ceramics, alloys, polymers and composites. Corrosion is a significant issue in the fabrication and selection of metals and alloys for service *in vivo* [1, 2]. Implant loosening and failure may occur due to various corrosion mechanisms in the oral environment [3, 4]. Stainless steel includes a wide range of steel types suitable for corrosion or oxidation resistance applications in different environments [5-7]. In the field of biomaterial industry, stainless steel and ceramics have been successfully used in advanced medical devices and implants [8]. Yttria-stabilized zirconia (YSZ) is an advanced ceramic material that exhibits excellent properties like low thermal conductivity, very high thermal stability, mechanical strength and fracture toughness [9, 10].

YSZ nanomaterials are used in biomedical and orthopaedic applications, mainly for repair and replacement of damaged parts of bones, human skeleton, joints and teeth due to their good biocompatibility, osseointegration, and bio inertness. YSZ are also used as catalysts [11, 12].

Chitosan is a biodegradable biopolymer, N-deacetylated product of chitin. It is highly hydrophobic and insoluble in water [13], but soluble in dilute organic acids such as acetic acid [14]. It possesses a regenerative effect on connective gum tissue and accelerates the formation of osteoblast responsible for bone formation. In addition, it has antimicrobial property that helps to protect the host from infection. Due to this property, it is widely used in dental applications. The chitosan thin film developed on the surface of ceramic-coated metal surfaces leads to the formation of a bio composite layer. This bio composite chitosan layer stops the various ions present in saliva from attacking the coating and on the other hand it accelerates the development of osteoblast responsible for new bone formation. The chitosan coated dental implants possess high biocompatibility [15].

Electrophoretic deposition (EPD) is a fast and cost-effective method to obtain a high-purity layer of desired thickness. This coating technique provides more uniform particle distribution compared to other conventional methods like electro deposition, dip coating, spin coating, plasma spray and ion beam coating. This technique is based on the electrophoresis mechanism in which the charged particles move from the suspension to the metal surface in an electric field yielding a thin uniform deposit on a substrate under various surfaces [16, 17]. The dip coating method is the most reliable method compared to other coating methods as it requires less time and simple low-cost equipment. Coating thickness depends on time and viscosity of the solution and it is optimized by changing the concentration of solution and time [18-20].

* To whom all correspondence should be sent:
E-mail: mohandoss.s@rajalakshmi.edu.in

The nanocomposite coating embedded in YSZ and chitosan (CS) protects the 316L SS against aggressive ions attacks from the oral environment and chitosan resists bacterial attacks from different foodstuffs [21, 22].

EXPERIMENTAL

Materials

Chitosan (degree of deacetylation 100), nano YSZ (99.99%) (particle size <100 nm) were obtained from Thermo Fisher Scientific. The IPA solvents, acetic acid and artificial saliva substances used were of AR grade.

Substrate preparation

ASTM F-89 standard 316L stainless steel (316L SS) (sized 10×10×2 mm) was used as a working electrode after polishing it mechanically using grit silicon carbide papers followed by gentle wash in dilute HCl and soap solution. Further, the samples were ultrasonically cleaned and oven dried. The dried 316L SS substrates were stored in desiccators prior to the EPD process. The chemical composition of 316L SS and 314 SS is given in Table 1.

Nano YSZ suspension preparation

2% nano YSZ suspension was prepared by mixing of 2g nano YSZ powder in isopropyl alcohol. In order to get an agglomerate-free suspension an ultrasonication process was carried out for about 10 minutes.

Chitosan solution preparation

2 % chitosan solution was prepared by mixing of finely ground 2g of chitosan flakes in 2% glacial acetic acid. The resultant solution was stirred constantly for 10 hours. The obtained homogeneous solution was stored in a cool place [23].

Nano YSZ deposition on metal substrate by EPD process

316L SS (sized 10×10×2 mm) was used as working electrode and a thin plate of 314 SS was used as anode. About 1 cm distance was maintained between the two electrodes. The working electrode was covered on one side with non-conducting Teflon tape and the covered part was immersed in the 2% nano YSZ suspension so that only the uncovered substrate faced in front of the anode can be coated. During the EPD process, the YSZ suspension was gently stirred. Deposition was carried out on a 1 cm^2 surface area with an applied potential of 70V at a constant time of 5 minutes. The obtained nano YSZ coating was gently taken out from bath and dried at room temperature for 5 minutes followed by air sintering at 800°C. The structural and morphological properties of the obtained samples were determined.

Chitosan coating on nano YSZ surface by dip coating

The chitosan solution was freshly prepared and nano YSZ coated 316L SS samples were dipped for 1 to 5 minutes. All the specimens were then gently removed from the chitosan bath. The obtained chitosan-coated samples were dried at room temperature.

Artificial saliva (AS) preparation

AS was prepared according to the literature reported [24]. Briefly, methyl-p-hydroxybenzoate (MPS) (2.00 g), sodium carboxymethyl cellulose (10.00 g), potassium chloride (0.625 g), magnesium chloride hexahydrate (0.059 g), calcium chloride dihydrate (0.166 g), potassium hydrogen phosphate (0.804 g), potassium dihydrogen phosphate (0.326 g) were mixed together in one liter of double distilled water. Finally, the pH of AS was adjusted to 6.75 using KOH solution.

Characterization

The microstructure and uniformity of nano chitosan/YSZ was investigated using FESEM (Carl Zeiss). Bruker model was used to obtain XRD patterns of nano chitosan/YSZ. Electrochemical workstation (Bio Logic SP240) was used to investigate electrochemical impedance. Five samples were analyzed for each OCP, CPP and impedance studies. The cell viability of all samples was analysed by the MTT assay method.

Table 1. Chemical composition of 316L SS and 314 SS

Element	% C	% Cr	% Ni	% Mn	% Mo	% P	% Si	% S	% Fe
316L SS	0.03	17.8	14.2	2.0	2.28	0.025	0.72	0.03	62.915
314L SS	0.26	24.6	21.8	2.0	-	0.045	2.10	0.03	49.165

RESULTS AND DISCUSSION

Micro hardness studies

Figure 1 presents the micro hardness of bare 316L SS and nano bio composite coated on 316L SS. A constant load of 100 g was applied on the specimen to check the micro hardness. The bio composite layer displays a higher hardness value (355 HV) compared to uncoated specimen (157 HV). This analysis confirms that the bio composite layer possesses high mechanical strength and high stability compared to nano YSZ coated and uncoated specimen [25].

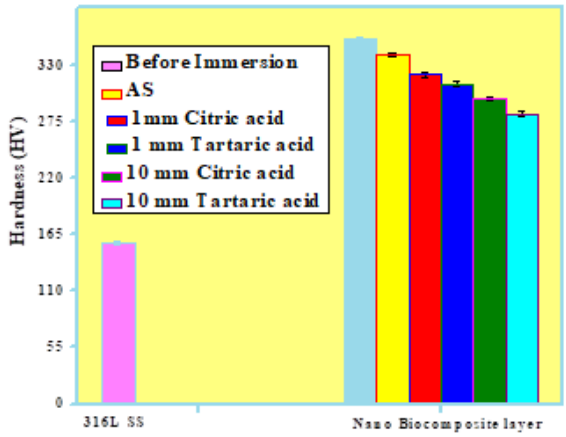

Figure 1. Micro hardness of bare 316L SS and nano biocomposite layer coated on 316L SS before immersion in AS, AS, AS + 1 mm citric acid, AS + 1 mm tartaric acid, AS + 10 mm citric acid and AS + 10 mm tartaric acid, respectively.

X-ray diffraction studies (XRD)

Figure. 2 presents the XRD pattern of the nano biocomposite layer coated on 316L SS before immersion in AS, AS, AS + 1 mm citric acid, AS + 1 mm tartaric acid, AS + 10 mm citric acid and AS + 10 mm tartaric acid. The XRD data confirm the presence of chitosan and nano YSZ and the diffraction patterns matched with JCPDS file No. 82-1246 and 79-0418. The intense peaks appearing at 2θ = 11, 19.8, confirm the crystalline nature of chitosan and those at 30.2, 50.4 and 60.0 confirm the crystalline nature of nano YSZ [26, 27] without any impurities in the coatings.

Fourier transform infrared spectroscopy (FT-IR)

The FTIR spectra of the nano biocomposite layer coated on 316L SS before immersion in AS, AS + 1 mm citric acid, AS + 1 mm tartaric acid, AS + 10 mm citric acid and AS + 10 mm tartaric acid are presented in Figure. 3.

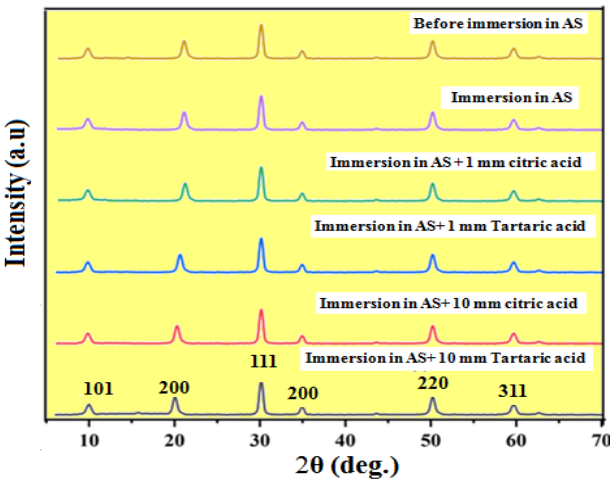

Figure 2. X-ray diffraction of nano biocomposite layer coated on 316L SS in before immersion in AS, AS, AS + 1 mm citric acid, AS + 1 mm tartaric acid, AS + 10 mm citric acid and AS + 10 mm tartaric acid, respectively.

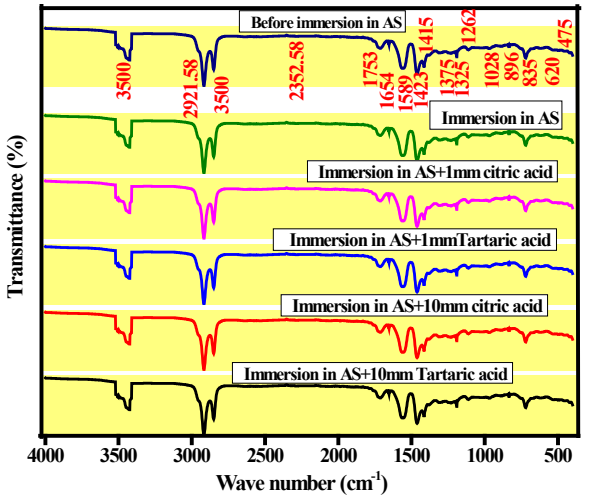

Figure 3. FTIR spectra of nano biocomposite layer coated on 316L SS in before immersion in AS, AS, AS + 1 mm citric acid, AS + 1 mm tartaric acid, AS + 10 mm citric acid and AS + 10 mm tartaric acid, respectively.

Strong and weak FTIR peaks are observed within the range of 3500-1000 cm^{-1}. The peaks at 3500, 2921, 1589 and 1423 cm^{-1} are attributed to the presence of O-H, C-H, N-H, C-O-C and C-N bonds of chitosan, respectively [28, 29]. The peaks at 636 cm^{-1} indicate the presence of nano YSZ along with chitosan.

The nano YSZ coating was made by an EPD process and chitosan was coated on nano YSZ surface by dip coating. The uniformity and crack-free nature of the nano chitosan /YSZ bio composite coating was observed using optical microscope and FESEM. The observed results for optical microscopic image and FESEM image of nano chitosan /YSZ are depicted in Figure 4.

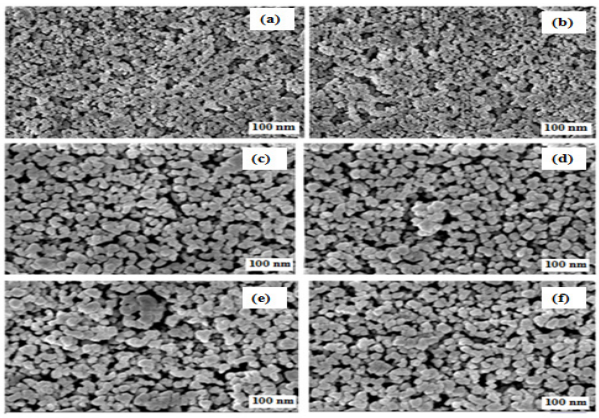

Figure 4. FESEM images of the nano biocomposite layer coated on 316L SS before immersion in AS, AS, AS + 1 mm citric acid, AS + 1 mm tartaric acid, AS + 10 mm citric acid and AS + 10 mm tartaric acid, respectively.

These images confirm the uniform, crack-free nature of nano chitosan/YSZ. This study further confirms that the nano biocomposite coatings are composed of 40 -80 nm grain sized YSZ and 80-200 nm grain sized chitosan.

EDAX analysis was helpful to identify the elemental composition of nano chitosan /YSZ. The presence of C, O, Y, Zr and N in chitosan and nano YSZ without any impurity is shown in Figure. 5.

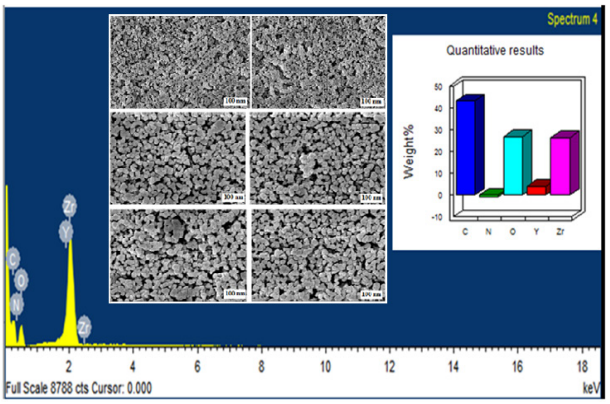

Figure 5. EDAX spectrum of nano bio composite coated on 316L SS

This study further confirms the absence of oxidized products of the base metal (iron oxide) during the sintering process and also the lack of decomposition of chitosan and nano YSZ during EPD and dip coating process.

Electrochemical studies

Open circuit potential (OCP). The OCP time measurement results [30] of nano biocomposite layers with various concentrations of (a) AS + 1 mm citric acid (b) AS + 1 mm tartaric acid (c) AS + 10 mm citric acid (d) AS + 10 mm tartaric acid and uncoated 316L SS are presented in Figure. 6. The OCP studies of all samples were carried out at different concentrations for about 1 hour. A nobler shift was observed for nano biocomposite coated samples in all media when compared to the uncoated 316L SS sample indicating the better corrosion resistance of the nano biocomposite layer. On adding different concentrations of citric acid and tartaric acid to AS the OCP values slightly decreased due to biofilm-acid interaction.

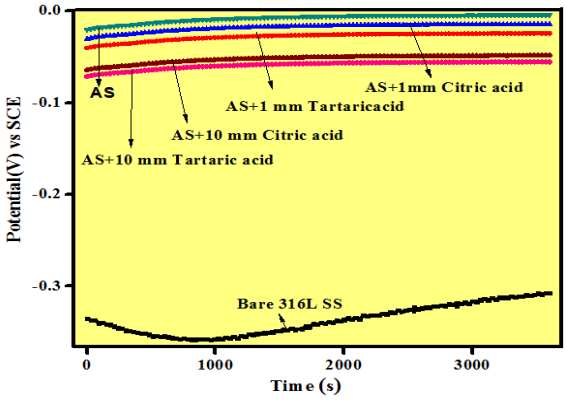

Figure 6. Open circuit potential time measurement for uncoated and nano biocomposite layer coated on 316L SS in (a) AS + 1 mm citric acid (b) AS + 1 mm tartaric acid (c) AS + 10 mm citric acid (d) AS + 10 mm tartaric acid, respectively.

Electrochemical impedance studies (EIS). EIS studies were carried out for all specimens under OCP conditions after immersion in various concentrations of AS + 1 mm citric acid, AS + 1 mm tartaric acid, AS+10 mm citric acid, AS+10 mm tartaric acid and uncoated 316L SS in the frequency range from 10 kHz to 10 mHz. EIS and the corresponding equivalent circuit results are presented in Figure 7.

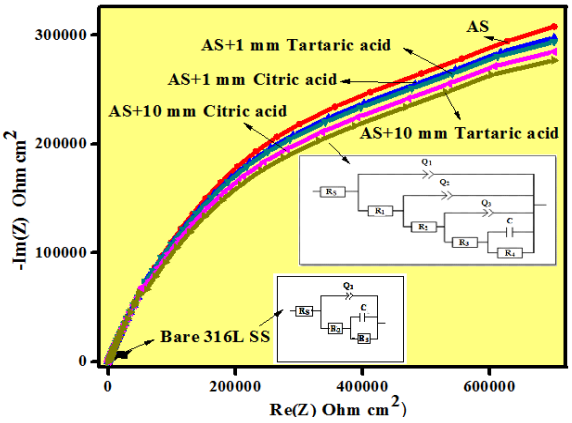

Figure 7. Nyquist plot obtained for uncoated and nano biocomposite layer coated on 316L SS in AS, AS + 1 mm citric acid, AS + 1 mm tartaric acid, AS + 10 mm citric acid and AS + 10 mm tartaric acid, respectively.

Nano biocomposite layer coated 316L SS for about 3 minutes possesses maximum impedance (30 MΩ cm^{-2}) compared to other coated samples and uncoated 316L SS.

The electrochemical parameters were obtained by Z Sim curve fitting analysis where, Rs is solution resistance, R_1 and Q_1 corresponding polarization resistance and constant phase element (CPE) of nano YSZ coated layer. R_2 and Q_2 represent corresponding polarization resistance and CPE of passivation layer on metal surface, R_3 and C correspond to resistance and capacitance of metal surface. In Figure 7 Rs represents solution resistance, R_1 and Q_1 correspond to polarization resistance and CPE of chitosan layer. R_2 and Q_2 represent corresponding polarization resistance and CPE of nano YSZ layer. R_3 and Q_3 depict polarization resistance and CPE of passivation layer, R_4 and C represent polarization resistance and capacitance of passivation layer. The obtained results are presented in Table 1.

The chitosan barrier resistance (R_{b1}) and passivation resistances (Rp) of biocomposite layer coated for about 3 minutes was maximum compared to uncoated 316L SS. The charge transfer resistance of the uncoated specimen was much less than that of nano biocomposite layer and uncoated metal. This indicates that nano biocomposite layer possesses higher resistivity toward aggressive ions attack from AS medium and it does not allow electron transfer from the metal surface to the bulk of AS medium.

Bode impedance and Bode phase plots of biocomposite layer in AS, AS + 1 mm citric acid, AS + 1 mm tartaric acid, AS + 10 mm citric acid, AS + 10 mm tartaric acid and uncoated 316L SS are given in Figure 8 (a, b). Maximum impedance values are observed for biocomposite layer coatings for about 3 minutes when compared to uncoated 316L SS specimens.

Table 1. Z fit values of nano biocomposite coated samples in AS medium along with citric and tartaric acid and comparison with uncoated 316L SS

Acid concentration	|Z| Ω cm^2	R_S Ωcm^2	Q_{coat} (F cm^{-2}s^n)	n_{coat}	R1 (chitosan layer)	R2 YSZ coat	Q_b (F cm^{-2}s^n)	n_b	R3 Ω cm^2	C_{dl} F cm^2	R4 Ωcm^2
Uncoated 316L SS	5644	388	----	0.81	----	----	----	----	190	3.933×10^{-5}	534.5
AS	308078	20.5	8.19×10^{-11}	0.28	5.48×10^{6}	2.06×10^{6}	7.51×10^{-10}	0.22	1.20×10^{6}	9.52×10^{-11}	184484
AS+1mm citric acid	295578	27.8	6.59×10^{-11}	0.30	5.76×10^{6}	1.64×10^{6}	6.89×10^{-10}	0.24	0.98×10^{6}	8.92×10^{-11}	164504
AS+1mm tartaric acid	299078	24.5	7.49×10^{-11}	0.32	5.88×10^{6}	1.86×10^{6}	7.01×10^{-10}	0.26	1.01×10^{6}	9.04×10^{-11}	168424
AS+10mm citric acid	293578	30.8	5.96×10^{-11}	0.33	5.24×10^{6}	1.48×10^{6}	6.64×10^{-10}	0.29	0.86×10^{6}	8.42×10^{-11}	158400
AS+10mm tartaric acid	291278	32.9	5.43×10^{-11}	0.35	5.08×10^{6}	1.24×10^{6}	6.21×10^{-10}	0.31	0.78×10^{6}	8.34×10^{-11}	152444

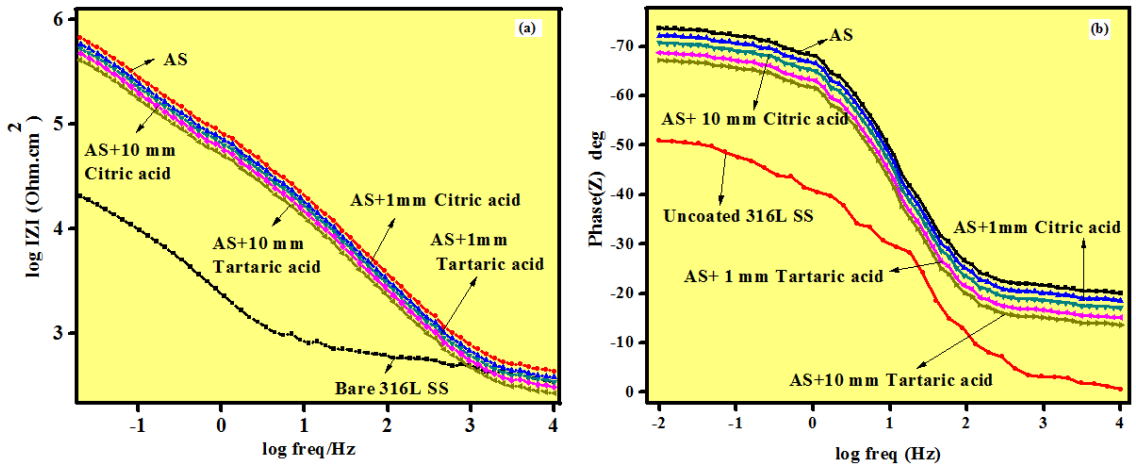

Figure 8. (a) Bode impedance (b) Bode phase plots obtained for uncoated and nano biocomposite layer coated on 316L SS in AS, AS + 1 mm citric acid, AS + 1 mm tartaric acid, AS + 10 mm citric acid and AS + 10 mm tartaric acid, respectively.

The shape of the phase angle *vs.* frequency relationship indicates the capacitive behavior of the coatings. The phase angle of the biocomposite layer displays a significant shift to −70° and this result confirms that the biocomposite layer exhibits a highly capacitive behavior compared to all other specimens. It was also observed that the corrosion resistivity of the biocomposite layer was significantly higher than that of uncoated 316L SS samples [31, 32].

Cyclic potentiodynamic polarization

The cyclic potentiodynamic polarization studies were carried out for all specimens with various concentrations of AS, AS+ 1 mm citric acid, AS + 1 mm tartaric acid, AS + 10 mm citric acid, AS + 10 mm tartaric acid and uncoated 316L SS and the obtained results are presented in Figure. 9.

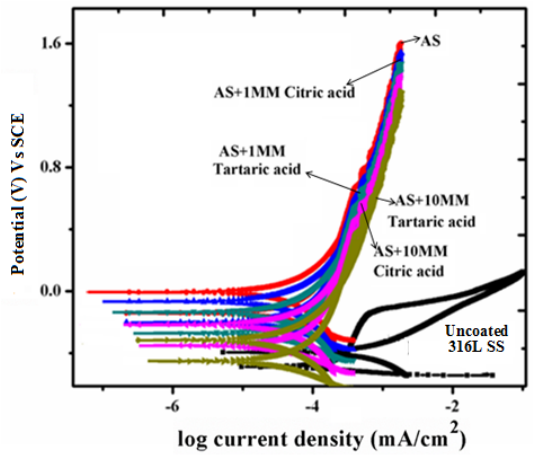

Figure 9. Cyclic potentiodynamic polarisation curves obtained for uncoated and nano biocomposite layer coated on 316L SS in AS, AS + 1 mm citric acid, AS + 1 mm tartaric acid, AS + 10 mm citric acid and AS + 10 mm tartaric acid, respectively.

The parameters obtained from the polarization curve are corrosion potential (Ecorr) and corrosion current density (Icorr). The Ecorr and Icorr values were determined by Tafel slope extrapolation, and the passive current density was obtained from the passive zone where the corrosion current remained approximately constant. The corrosion potential (E_{corr}) and corrosion current density (I_{corr}) values are given in Table 2. The nano biocomposite layer coated for 3 minutes possesses a higher corrosion potential E_{corr} -172.569 mV and a lower corrosion current density I_{corr}0.001µA value among all specimens. The E_{corr} values are shifted in less negative direction from uncoated sample to chitosan coated sample. This is due to the stable nature of the nano biocomposite layer toward aggressive ions attacks from the AS medium and this layer stops the release of ions from substrate to solution. Corrosion rate can be calculated by using ASTM-G 102-89 standard equation:

$$\text{Corrosion rate(CR)} = \frac{\text{K1}\times \text{Icorr}}{\rho}\times \text{EW mm/year}$$

where, CR is corrosion rate, EW is equivalent weight of the metal, ρ is density, K1 = 3.27 × 10^{-3}, Icorr is corrosion current. These results indicate that nano biocomposite layers on the metal surface are more stable and possess better barrier property compared to uncoated 316L SS.

Table 2. Tafel fit values of nano biocomposite coated samples in AS medium along with citric and tartaric acid and comparison with uncoated 316L SS.

AS and acid concentration	$E_{corr\ (mV)}$ *vs* SCE	I_{corr} µAcm^{-2}
316L SS	-425	2.308
AS	-088	0.001
AS+1 mm citric acid	-105	0.003
AS+1 mm tartaric acid	-107	0.002
AS+10 mm citric acid	-110	0.004
AS+10 mm tartaric acid	-115	0.005

Biocompatibility studies

The cytotoxicity studies of uncoated 316L SS, nano biocomposite coated 316L SS samples immersed in AS, AS+1 mm citric acid, 1 mm tartaric acid, 10 mm citric acid and 10 mm tartaric acid are shown in Figures 10 and 11, respectively. These studies were carried out using human MG-63 osteoblast cell line by MTT assay method [28]. Most of the human MG-63 osteoblast cell line were viable on nano chitosan /YSZ coated 316L SS rather than nano YSZ and 316L SS samples. Hence, the cell viability of nano chitosan /YSZ coated sample was found to be highly uniform and non-porous coating on the metal surface [33].

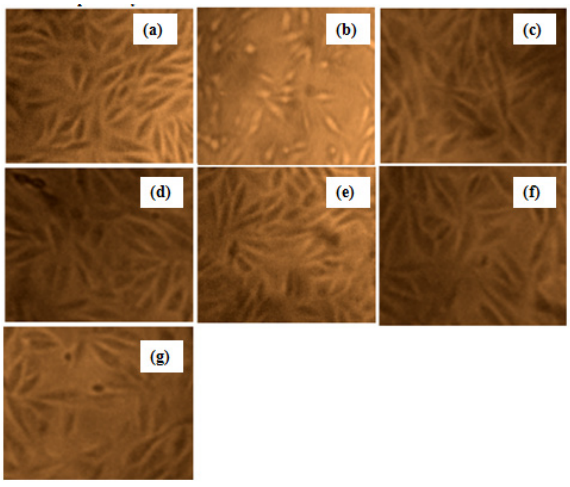

Figure 10. (a),(b),(c),(d).(e),(f) and (g) Microscopic images of Cell for control cell line, uncoated, nano bio composite coated sample immersed in AS, AS+1 mm citric acid,1 mm tartaric acid, 10 mm citric acid and 10 mm tartaric acid.

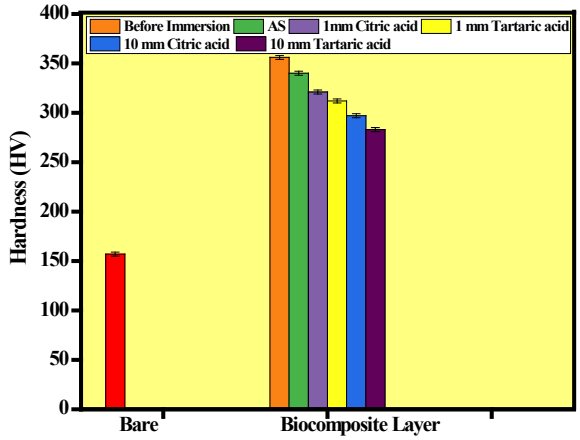

Figure 11. MTT assay results obtained for bare 316L SS compared with nano bio composite coated sample immersed in AS, AS+1 mm citric acid, 1 mm tartaric acid, 10 mm citric acid and 10 mm tartaric acid.

DISCUSSION

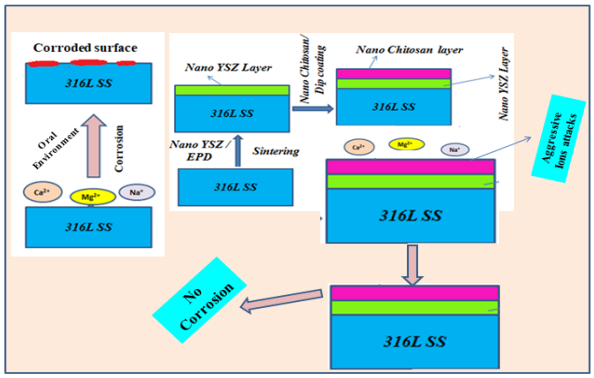

Figure 12. Schematic representation of the corrosion mechanism on the surface of bare 316L SS and biocomposite coated 316L SS.

Figure 12 is a schematic representation of the corrosion mechanism on the surface of bare 316L SS and biocomposite coated 316L SS and this paper deliberates the development of nano biocomposite coating by means of nano YSZ and nano chitosan along with determination of its surface morphology and electrochemical properties. Dip coating process was utilized to develop chitosan coatings on air sintered nano-YSZ coated 316L SS samples. The coated samples were characterized using XRD, FTIR, FESEM and EDAX in order to evaluate their structural, functional and morphological properties. Further, the optimized samples were subjected to electrochemical studies in artificial saliva medium in the presence of various concentrations of citric acid and tartaric acid which was not reported earlier by any researchers using this bio composite. In our previous research work nano YSZ alone was coated on the surface of 316L SS but in the present work a nano biocomposite is coated on the surface of 316L SS. The hardness, electrochemical characteristics OCP, CPP and electrochemical impedance studies confirmed that the biocomposite coated 316L SS samples possess very good corrosion resistance in artificial saliva medium. The OCP value moves in nobler direction when compared with nano YSZ coatings. The Nyqust value and Bode impedance value also confirm the above statement. The Ecorr and Icorr values also confirm that the biocomposite coated samples possess better corrosion resistivity than nano YSZ coated samples. The obtained results for the optimized sample using citric and tartaric acid depict a better electrochemical performance compared to uncoated 316L SS in artificial saliva medium.

CONCLUSIONS

Nano YSZ coating on 316L SS was obtained by electrophoretic deposition and chitosan film was formed on the nano YSZ by dip coating. FESEM studies confirmed that YSZ particles deposited on 316L SS were in the nano scale range (40-80 nm) roughly spherical; chitosan size was in the 80-200 nm range. Electrochemical studies of the bio nanocomposite revealed its higher corrosion resistance compared to nano YSZ/316L SS and bare metal substrate. OCP studies indicated that the bio nanocomposite coated samples shifted in nobler direction indicating that the bio nanocomposite film exhibited better polarization resistance and lower capacitance values as observed from EIS studies. Electrochemical studies revealed that the nano biocomposite layer could act as an effective barrier against corrosive ions attack and resist ions intercalation from artificial saliva of various composition. Chitosan is water-insoluble and possesses very good hydrophobicity. It hardly reacts with citric acid and tartaric acid in the oral environment at room temperature. As foodstuffs contain very little amounts of acids and the acids only contact with implants in few seconds, therefore this type of acids not readily attack the dental implants. The composite coatings enhanced the durability and stability of the base metal. Finally, the developed bio nanocomposite coated sample would be an ideal choice for dental implant applications.

Acknowledgement: *The authors are thankful to the University Grants Commission, India, for the financial support and encouragement (MRP-6134 (SERO/UGC).*

REFERENCES

1. N. Eliaz, *J. Mech. Behav. Biomed. Mater.*, **12,** 234 (2008).

2. G. Manivasagam, D. Dhinasekaran, A. Rajamanickam, *Recent Patents Corros. Sci.,* **2**, 40 (2010).
3. T. V. Thamaraiselvi, S. Rajeswari, *Trends Biomater. Artif. Organs,* **18,** 9 (2004).
4. C.Viazzi, J. P. Bonino, F. Ansart, *Surf. Coat. Technol*., **20**, 3889 (2006).
5. N. K. Sahoo, S. C. Anand, J. R. Bhardwaj, P. Sachdeva, B. L. Sapru, *Med. J. Armed Forces India*, **50** (1), 10 (1994).
6. R. N. Brown, B. E. Sexton, M. G. Chu, T. R. Katona, K. T. Stewart, H. M. Kyung, S. S. Liu, *Am. J. Orthod.* **145**(4), 496 (2014).
7. P. M. Hashemi, E. Borhani, M. S. Nourbakhsh, *Nanomed. J.,* **3**(4), 202 (2016).
8. M. Holzapfel, *Drug Delivery Rev*., **65**, 581 (2013).
9. J. R. Kelly, I. Denry, *Dent. Mater*., **24**, 289 (2008).
10. X. Y. Gu, X. Li, Q. Liu, Y.X. Chen, Y. Li, *Mater. Eng*., **38**, 1044 (2009).
11. C. Viazzi, J. P.Bonino, F. Ansart, Surf. Coat. Technol. 201, 3889, (2006). **Same as ref. 4**
12. T. V.Thamaraiselvi, S. Rajeswari, *Trends Biomater. Artif. Organs,* **18**, 9 (2004).
13. D. E. Ali-Komi, M. R. Hamblin, *Int. J. Adv. Res.,* **4**(3), 411 (2016).
14. Q. Y. Deng, Ch. R. Zhou, B. H. Luo, *Pharmaceutical Biology*, **44**(5), 336 (2006).
15. Sh. H. Hsu, H. J. Tseng, T. L. Tsou, H. J. Wang, *Journal of Tissue Engineering and Regenerative Medicine*, **7**(1), 20 (2013).
16. L. Besra, M. Liu, *Prog. Mater. Sci*., **52**, 1 (2007).
17. M. Boehmer, *Langmuir,* **12**, 5747 (1996).
18. M. Nakashima, T. Ebine, M. Shishikura, K. Hoshino, K. Kawai, K. Hatsusaka, *Mater. Interfaces*, **2**(5), 1471 (2010).
19. M. Deepa, T. K.Saxena, D. P. Singh, K. N. Sood, S. A. Agnihotry, *Electrochim Acta,* **51**,1974 (2006).
20. S. Patil, U. Hoshing, D. Rachalwar, *Journal of Current Research,* **9**(11), 61490 (2017).
21. S. Singh, G. Singh, K. Aggarwal, *International Journal of Biological Macromolecules,***151**, 519 (2020).
22. S. Singh, G. Singh, N. Bala, *Materials Chemistry and Physics,* **237**,121884 (2019).
23. A. Domard, M. Rinaudo, *International Journal of Biological Macromolecules,* **5**(1), 49 (1983).
24. S. Patil, U. Hoshing, D. Rachalwar, *Journal of Current Research*, **9** (11), 61490 (2017).
25. V. M. Matyunin, A. Yu. Marchenkov, A. N. Demidov, *Materials Science and Engineering Metals Tech*., **6**, 53 (2013).
26. M. N. Tsampas, F. M. Sapountzi, P. Vernoux, *Catalysis Science & Technology,* **5**(11), 4884 (2015).
27. J. A. M. Oliveira, R. A. C. De Santana, A. D. O. W. Wanderley, *Neto Progress in Organic Coatings.* **143**,105631, (2020).
28. T. Lertwattanaseri, N. Ichikawa, T. Mizoguchi, Y. Tanaka, S. Chirachanchai, *Carbohydrate Research,* **344**(3), 331 (2009).
29. K. Alagarsamy, V. Vishwakarma, G. S. Kaliaraj, N. C. Vasantha, S. J. R. Samuel, *Journal of Adhesion Science and Technology*. **34**(4), 349 (2020).
30. Ch. Chen, J. Zuo, Y. Wang, *Int. J. Electrochem. Sci*., **15**, 4944 (2020).
31. J. M. Bastidas, J. L. Polo, C. L. Torres, E. Cano, *Corrosion Science,* **43**(2), 269 (2001).
32. D. Predo, S. L. Iconar, M. V. Predoi, *Coatings,* **10**(905), 1 (2020).
33. W. Jun, Ch. Peng, J. Wen, G. Mingzhi, *Biomedical Research***, 289**(10), 1 **(**2017).